

Photoinduced Electron-Transfer Degenerate Cope Rearrangement of 2,5-Diaryl-1,5-hexadienes: A Cation-Radical Cyclization–Diradical Cleavage Mechanism

Hiroshi Ikeda,[†] Tomonori Minegishi,[†] Hideyuki Abe,[†] Akinori Konno,[†]
Joshua L. Goodman,[‡] and Tsutomu Miyashi^{*,†}

Contribution from Department of Chemistry, Graduate School of Science, Tohoku University, Sendai 980-77, Japan, and Department of Chemistry, University of Rochester, Rochester, New York 14627

Received June 10, 1997[⊗]

Abstract: Under the 9,10-dicyanoanthracene (DCA)-sensitized photoinduced electron-transfer (PET) conditions, 2,5-diaryl-3,3,4-tetradeuterio-1,5-hexadiene (d_4 -**1**) undergoes a degenerate Cope rearrangement to give a photostationary mixture of d_4 -**1** and its 1,1,6,6-tetradeuterio analogue d_4 -**1'** in 52:48. This reaction involves 1,4-diaryl-2,2,3,3-tetradeuteriocyclohexane-1,4-diyl cation radical (d_4 -**2**⁺), which can be captured by molecular oxygen as 1,4-diaryl-2,3-dioxabicyclo[2.2.2]octane (**3**). In contrast, nonphotoinduced electron-transfer (non-PET) reaction of d_4 -**1** with cerium(IV) ammonium nitrate similarly forms d_4 -**2**⁺, but the degenerate Cope does not take place. This observed striking contrast between PET and non-PET was ascribed to the formation of 1,4-diaryl-2,2,3,3-tetradeuteriocyclohexane-1,4-diyl (d_4 -**2**) in the PET process by back-electron transfer from DCA^{•-} to d_4 -**2**⁺. The results of similar PET and non-PET reactions of 1,4-diphenyl-2,3-diazabicyclo[2.2.2]-oct-2-ene (**4c**) and its 5,5,6,6-tetradeuterio analogue (d_4 -**4c**) support this conclusion. Photoacoustic calorimetry of the PET reaction of 2,5-diphenyl-1,5-hexadiene (**1c**) suggests that 1,4-diphenylcyclohexane-1,4-diyl (**2c**) lies *ca.* 18.8 kcal/mol higher in energy than **1c** and *ca.* 25.6 kcal/mol below the ion-radical pair [**2c**⁺/DCA^{•-}]. Deazetation of d_4 -**4c** demonstrates that d_4 -**2c** undergoes cleavage to d_4 -**1c** and d_4 -**1c'** with bond-breaking kinetic isotope effects, $k(d_4$ -**2c**)^{H4} / $k(d_4$ -**2c**)^{D4} = 1.11, completing a cation-radical cyclization–diradical cleavage mechanism.

Introduction

Upon heating, acyclic 1,5-hexadienes undergo the Cope rearrangement, which is an extremely useful thermal rearrangement in organic synthesis, and the rearrangement occurs stereospecifically through a chair six-membered cyclic transition state. The reaction is characterized by large negative entropy of activation and is relatively insensitive to substituent and solvent effects.¹ In fact, most Cope rearrangements display these characteristics and have been accounted for consistently by a concerted mechanism. However, a stepwise cyclization–

cleavage (CY–CL) mechanism through a chair cyclohexane-1,4-diyl intermediate has been argued as one possible nonconcerted mechanism.^{2,3} Dewar previously proposed that this mechanism would operate in the Cope rearrangement of the labeled 2,5-diphenyl-1,5-hexadiene (d_4 -**1c'**) through a 1,4-diphenylcyclohexane-1,4-diyl intermediate (d_4 -**2c**) (Scheme 1a).^{3f} Although no direct experimental evidence for the intermediacy of d_4 -**2c** is reported yet, Doering's recent theoretical calculation for the enthalpy of formation of diyl **2c** and the “frustrated” Cope rearrangement of 2,6-diphenyl-1,6-heptadiene^{2b} are intriguing results to assert a possible operation of a CY–CL mechanism in the thermal Cope rearrangement of d_4 -**1c**.

On the other hand, Bauld and co-workers have theoretically argued a cation radical (CR) variant⁴ of a thermal CY–CL process. Their calculation suggests that the parent 1,5-hexadiene CR would cyclize either to a chair or to a boat cyclohexane-1,4-diyl CR intermediate with a low energy barrier, but the second cleavage step would require a relatively high activation, suggesting that the CR cleavage is a crucial key step in a cation-radical cyclization–cation-radical cleavage (CRCY–CRCL) mechanism (Scheme 1b). Independent of this theory, we investigated the 9,10-dicyanoanthracene (DCA)-sensitized photoinduced electron-transfer (PET) reaction of d_4 -**1** to examine if the PET degenerate Cope rearrangement proceeds through a cyclohexane-1,4-diyl CR intermediate.⁵ Under DCA-sensitized conditions, the degenerate Cope of d_4 -**1** occurs efficiently, giving

(4) Bauld, N. L.; Bellville, D. J.; Pabon, P.; Chelsky, R.; Green, G. *J. Am. Chem. Soc.* **1983**, *105*, 2378–2382. Bauld, N. L. In *Advances in Electron Transfer Chemistry*; Mariano, P. S., Ed.; JAI: London, 1992; Vol. 2; pp 1–66. See also ref 7f.

* To whom correspondence should be addressed.

[†] Tohoku University.

[‡] University of Rochester.

[⊗] Abstract published in *Advance ACS Abstracts*, December 15, 1997.

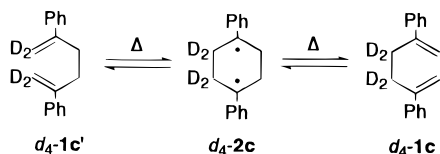
(1) See reviews, for instance: Rhoads, S. J.; Raulins, N. R. In *Organic Reactions*; Dauben, W. G., Ed.; Wiley: New York, 1975; Vol. 22, pp 1–252. Hill, R. K. In *Comprehensive Organic Synthesis*; Trost, B. M., Ed.; Pergamon: New York, 1991; Vol. 5, pp 785–826. Berson, J. A. In *Rearrangements in Ground and Excited States*; Mayo, P. d., Ed.; Academic: New York, 1980; Vol. 1, pp 311–390.

(2) (a) Doering, W. v. E.; Toscano, V. G.; Beasley, G. H. *Tetrahedron* **1971**, *27*, 5299–5306. (b) Roth, W. R.; Lennarts, H.-W.; Doering, W. v. E.; Birladeanu, L.; Guyton, C. A.; Kitagawa, T. *J. Am. Chem. Soc.* **1990**, *112*, 1722–1732.

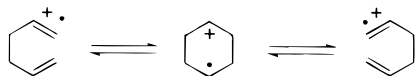
(3) (a) Dewar, M. J. S.; Wade, L. E. *J. Am. Chem. Soc.* **1973**, *95*, 290–291. (b) Dewar, M. J. S.; Ford, G. P.; McKee, M. L.; Rzepa, H. S.; Wade, L. E. *J. Am. Chem. Soc.* **1977**, *99*, 5069–5073. (c) Dewar, M. J. S.; Leslie E. Wade, J. *J. Am. Chem. Soc.* **1977**, *99*, 4417–4424. (d) Dewar, M. J. S. *J. Am. Chem. Soc.* **1984**, *106*, 209–219. (e) Dewar, M. J. S.; Healy, E. F. *Chem. Phys. Lett.* **1987**, *141*, 521–524. (f) Dewar, M. J. S.; Jie, C. *J. Am. Chem. Soc.* **1987**, *109*, 5893–5900. (g) Dewar, M. J. S.; Jie, C. *J. Chem. Soc., Chem. Commun.* **1987**, 1451–1453. (h) Dewar, M. J. S.; Jie, C. *Acc. Chem. Res.* **1992**, *25*, 537–543.

Scheme 1

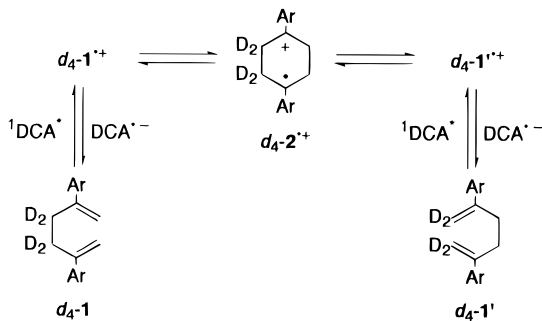
(a) Cope: A Hypothetical CY–CL Mechanism



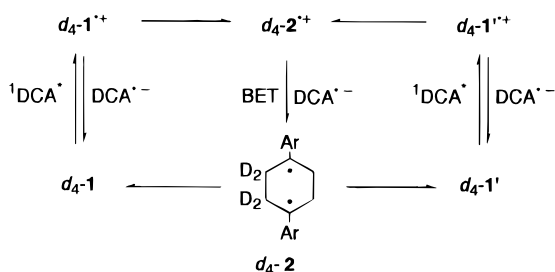
(b) CR Cope: A CRCY–CRCL Mechanism



(c) PET Cope: A CRCY–CRCL Mechanism



(d) PET Cope: A CRCY–DRCL Mechanism



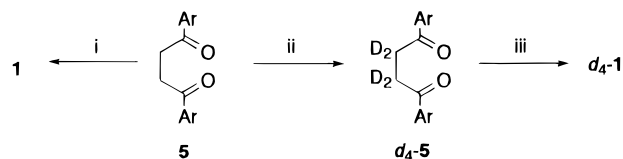
a: Ar = 4-MeOC₆H₄, b: Ar = 4-MeC₆H₄, c: Ar = C₆H₅, d: Ar = 4-ClC₆H₄

rise to a photostationary (PS) mixture of *d*₄-1 and the 1,1,6,6-tetradeuterio analogue (*d*₄-1'). The degenerate Cope rearrangement of *d*₄-1, however, did not take place in non-PET reactions such as a single-electron transfer with cerium(IV) ammonium nitrate (CAN). In order to gain insight into the mechanism of the PET degenerate Cope, 1,4-diphenyl-2,3-diazabicyclo[2.2.2]oct-2-ene (**4c**) and its 5,5,6,6-tetradeuterio analogue (*d*₄-**4c**) were also subjected to similar PET and non-PET reactions. Diene **1c** was formed from **4c** under PET conditions but not under non-PET conditions. On the basis of those results, the cationic radical cyclization–diradical cleavage (CRCY–DRCL) mechanism (Scheme 1d) was proposed for the PET degenerate Cope. In addition, an energetic argument also favors a CRCY–DRCL

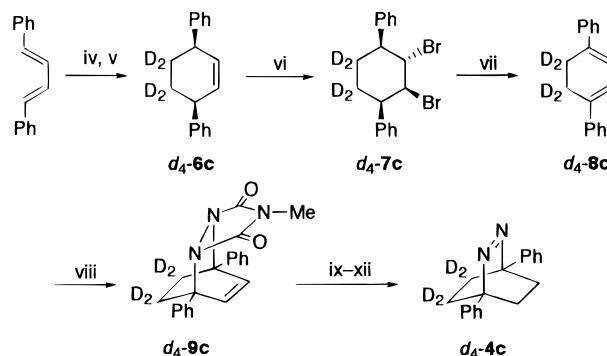
(5) Miyashi, T.; Konno, A.; Takahashi, Y. *J. Am. Chem. Soc.* **1988**, *110*, 3676–3677. A part of this work was presented at the XIIIth IUPAC International Symposium on Photochemistry (U.K., 1990).⁶

(6) Miyashi, T.; Ikeda, H.; Konno, A.; Okitsu, O.; Takahashi, Y. *Pure Appl. Chem.* **1990**, *62*, 1531–1538. For other experimental studies on the CR Cope rearrangement, see ref 7.

(7) (a) Lorenz, K.; Bauld, N. L. *J. Catal.* **1985**, *95*, 613–616. (b) Chen, G.-F.; Williams, F. J. *Chem. Soc., Chem. Commun.* **1992**, 670–672. (c) Miyashi, T.; Takahashi, Y.; Ohaku, H.; Ikeda, H.; Morishima, S. *Pure Appl. Chem.* **1991**, *63*, 223–230. (d) Ikeda, H.; Takasaki, T.; Takahashi, Y.; Miyashi, T. *J. Chem. Soc., Chem. Commun.* **1993**, 367–369. (e) Ikeda, H.; Oikawa, T.; Miyashi, T. *Tetrahedron Lett.* **1993**, *34*, 2323–2326. (f) Williams, F. J. *Chem. Soc., Faraday Trans.* **1994**, *90*, 1681–1687.

Scheme 2^a

a: Ar = 4-MeOC₆H₄, b: Ar = 4-MeC₆H₄, c: Ar = C₆H₅, d: Ar = 4-ClC₆H₄



^a Key: (i) Ph₃P⁺CH₃⁺I⁻, *t*-BuOK/THF; (ii) D₂O, Et₃N/dioxane; (iii) Ph₃P⁺CH₃⁺I⁻, *n*-BuLi/THF; (iv) Mg*/THF; (v) 1,2-dichlorotetradeuterioethane; (vi) pyridinium bromide perbromide/AcOH; (vii) DBU/C₆H₆; (viii) 4-methyl-1,2,4-triazoline-3,5-dione/AcOEt; (ix) H₂/Pt–CaCO₃/AcOEt; (x) KOH/*i*-PrOH; (xi) CuCl₂/*i*-PrOH; (xii) NH₄OH.

mechanism rather than a CRCY–CRCL mechanism. Herein, we report characteristics and energetics of the PET degenerate Cope rearrangement of *d*₄-1 in detail.

Results and Discussion

Syntheses and Electron-Donating Properties of 1a–d, d₄-1a–d, 4c, and d₄-4c. The labeled and unlabeled 4-methoxyphenyl, 4-methylphenyl, phenyl, and 4-chlorophenyl derivatives of 2,5-diaryl-1,5-hexadienes (*d*₄-**1a–d** and **1a–d**) were prepared from *d*₄-**5a–d** and **5a–d**,^{8–11} respectively (Scheme 2). 1,4-Diphenyl-2,3-diazabicyclo[2.2.2]oct-2-ene (**4c**)¹² and the labeled *d*₄-**4c** were derived from 1,4-diphenylcyclohexa-1,3-diene (**8c**) and the labeled *d*₄-**8c**, respectively, as shown in Scheme 2. The labeled *d*₄-**6c** prepared by the reaction^{13a} of (*E,E*)-1,4-diphenyl-1,3-butadiene and 1,2-dichlorotetradeuterioethane using active Mg was converted to *d*₄-**8c** and *d*₄-**9c**. The deuterium incorporations in *d*₄-**1a–d** and *d*₄-**4c** were shown to be 98–99% (3.92–3.96 atom D per molecule at C-2 and C-3) and 97% (3.88 atom D per molecule at C-5 and C-6), respectively, by ¹H NMR (CW, FT) and MS analyses.

2,5-Diaryl-1,5-hexadienes (**1a–d**) and diazene **4c** are good electron donors, and their oxidation potentials, *E*^{ox}_{1/2}, are low enough to quench the excited singlet state of DCA (¹DCA*) exothermically. Free energy changes,¹⁴ Δ*G*, associated with the forward electron transfer are calculated according to the Rehm–Weller equation^{15ab} and are listed in Table 1 together with *E*^{ox}_{1/2} and the DCA-fluorescence quenching rate constants,

(8) Campaigne, E.; Foye, W. O. *J. Org. Chem.* **1952**, *17*, 1405–1412.

(9) Stetter, H.; Bender, H.-J. *Chem. Ber.* **1981**, *114*, 1266–1233.

(10) Bailey, P. S.; Lutz, R. E. *J. Am. Chem. Soc.* **1948**, *70*, 2412–2426.

(11) Conant, J. B.; Lutz, R. E. *J. Am. Chem. Soc.* **1923**, *45*, 1303–1307.

(12) Engel, P. S.; Nalepa, C. J.; Horsey, D. W.; Keys, D. E.; Grow, R. T. *J. Am. Chem. Soc.* **1983**, *105*, 7102–7107.

(13) (a) Rieke, R. D.; Xiong, H. *J. Org. Chem.* **1991**, *56*, 3109–3118. (b) Wu, T.-C.; Xiong, H.; Rieke, R. D. *J. Org. Chem.* **1990**, *55*, 5045–5051.

(14) Δ*G* (kcal/mol) = 23.06 [*E*^{ox}_{1/2}(substrate) – *E*^{red}_{1/2}(DCA) – *E*_{0–0}] – *e*²/*εr* where *E*^{red}_{1/2}(DCA) is –0.95 V, *E*_{0–0} is 2.91 eV in CH₂CN, and the coulombic term (*e*²/*εr*) was ignored after Farid's example.^{15c}

Table 1. Oxidation Potentials ($E_{1/2}^{\text{ox}}$) and Free Energy Changes (ΔG) Associated with Electron Transfer with $^1\text{DCA}^*$ and DCA-Fluorescence Quenching Rate Constants (k_q) for **1** and **4c**

sub	$E_{1/2}^{\text{ox}}$ (V)	ΔG^c (kcal/mol)	$10^{10}k_q$ ($\text{M}^{-1} \text{s}^{-1}$)		
			CH_3CN	CH_2Cl_2	C_6H_6
1a	+1.27	-15.9	2.0	1.5	1.1
1b	+1.54	-9.7	1.5	1.0	0.50
1c	+1.68	-6.5	1.2	0.36	0.06
1d	+1.71	-5.8	1.1	0.28	0.03
4c	+1.16, +1.39 ^b	-18.4	1.6	1.2	1.1

^a Vs SCE in CH_3CN , scan rate 100 mV s^{-1} . ^b In CH_2Cl_2 . ^c In CH_3CN .

k_q . In accord with the calculated thermodynamics, **1a–d** quench the DCA-fluorescence with nearly the same rate constants, k_q , close to the diffusion control rate constant, but in the less polar solvent dichloromethane and the nonpolar solvent benzene, rate constants decrease with an increase in oxidation potential of **1**. Rate constants, k_q , of highly electron-donating **1a** in the three solvents were nearly the same regardless of solvent polarity, but those of the less electron-donating **1b–d** decrease with a decrease in solvent polarity.

The DCA-Sensitized PET Degenerate Cope Rearrangement of d_4 -1 and Chemical Capture of 2^{*+} . According to theoretical arguments, the Cope rearrangement of the parent 1,5-hexadiene CR can be explained either by a concerted or by a stepwise mechanism. In the former process, a suprafacial–suprafacial pathway was suggested to be favored based on orbital-symmetry correlations,¹⁶ while in the latter process, the rearrangement would occur through the “long-bonded” boat-like or chair cyclohexane-1,4-diyl CR intermediate (Scheme 1b).⁴ If a stepwise process similar to the latter operates in the PET degenerate Cope rearrangement of d_4 -1 (Scheme 1c), we thought that a cyclohexane-1,4-diyl CR intermediate (d_4 - 2^{*+}) may be intercepted by molecular oxygen, as various other intriguing CR intermediates have been.¹⁷

First, we investigated the degenerate Cope rearrangement of d_4 -1 and oxygenation of **1** under various DCA-sensitized conditions. Irradiation ($\lambda > 360 \text{ nm}$) of DCA with d_4 -1 at 20 °C gives a PS mixture of d_4 -1 and d_4 -1' in acetonitrile, dichloromethane, and benzene as shown in Table 2. In dichloromethane, the Cope rearrangement of d_4 -**1b–d** occurs efficiently even at -80 °C. The PS ratios are nearly the same regardless of solvent polarity and the electron-donating nature of substrates. The average PS ratio observed for four aryl derivatives in three different solvents is approximately 52:48 at 20 °C. However, the quantum efficiency for the degenerate Cope rearrangement was strongly dependent upon solvent polarity and the electron-donating nature of the substrates. Quantum efficiencies, Φ_{cor} , corrected by quenching efficiencies, Q_e , are shown in Table 2. The Φ_{cor} tends to increase as solvent polarity and the electron-donating nature of substrates decrease, except for the least electron-donating substrates d_4 -**1d**.

(15) (a) Rehm, D.; Weller, A. *Isr. J. Chem.* **1970**, *8*, 259–271. (b) Weller, A. *Z. Phys. Chem. (Munich)* **1982**, *133*, 93–98. (c) Gould, I. R.; Ege, D.; Moser, J. E.; Farid, S. *J. Am. Chem. Soc.* **1990**, *112*, 4290–4301. (d) Niwa, T.; Kikuchi, K.; Matsushita, N.; Hayashi, M.; Katagiri, T.; Takahashi, Y.; Miyashi, T. *J. Phys. Chem.* **1993**, *97*, 11960–11964.

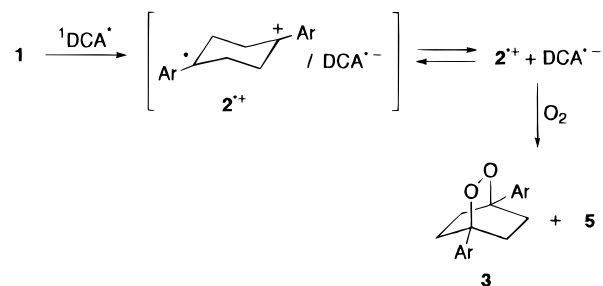
(16) Dunkin, I. R.; Andrews, L. *Tetrahedron* **1985**, *41*, 145–161.

(17) *Photoinduced Electron Transfer. Part C: Photoinduced Electron Transfer Reactions: Organic Substrates*; Fox, M. A., Chanon, M., Ed.; Elsevier: Amsterdam, 1988. Mizuno, K.; Pac, C. In *CRC Handbook of Organic Photochemistry and Photobiology*; Horspool, W. M., Song, P.-S., Eds.; CRC: New York, 1995; pp 358–374. Roth, H. D. In *Topics in Current Chemistry: Photoinduced Electron Transfer IV*; Mattay, J., Ed.; Springer-Verlag: Berlin, 1992; Vol. 163, pp 131–245. Lopez, L. In *Topics in Current Chemistry: Photoinduced Electron Transfer I*; Mattay, J., Ed.; Springer-Verlag: Berlin, 1990; Vol. 156, pp 117–166.

Table 2. Photostationary Ratio (d_4 -1: d_4 -1')^a and Corrected Quantum Yield (Φ_{cor}) for the PET Degenerate Cope Rearrangement of d_4 -1 at 20 °C

sub	d_4 -1: d_4 -1'			Φ_{cor}^e		
	CD_3CN	CD_2Cl_2	C_6D_6	CD_3CN	CD_2Cl_2	C_6D_6
d_4 - 1a	52:48 ^b	51:49 ^c	51:49 ^d	n.a. ^f	0.14	0.38
d_4 - 1b	53:47 ^c	52:48	54:46	0.21	0.32	0.48
d_4 - 1c	53:47	52:48	53:47	0.34	0.42	0.50
d_4 - 1d	52:48	53:47	53:47	0.33	0.36	0.35

^a [d_4 -1] = 100 mM. ^b [d_4 -1] = 1.25 mM. ^c [d_4 -1] = 50 mM. ^d [d_4 -1] = 25 mM. ^e $\Phi_{\text{cor}} = \Phi/Q_e$, where $Q_e = k_q\tau/[1]/(1 + k_q\tau[1])$ and [1] = 10 mM. ^f No attempt.

Scheme 3

a: Ar = 4-MeOC₆H₄, b: Ar = 4-MeC₆H₄, c: Ar = C₆H₅, d: Ar = 4-ClC₆H₄

Table 3. Solvent and Substituent Effects on the DCA-Sensitized Photooxygenation of **1**^a

sub	solvent	time (min)	conversion (%)	yields (%)	
				3	5
1a	C_6H_6	60	0	0	0
	CH_2Cl_2	5	37	37	0
1b	CH_2Cl_2	20	100	93	0
	CH_3CN^b	5	100	93	0
1c	CH_3CN	5	62	59	1
	CH_3CN	5	6	4	1
1d	CH_3CN	20	42	10	3
	CH_3CN	20	30	14	3

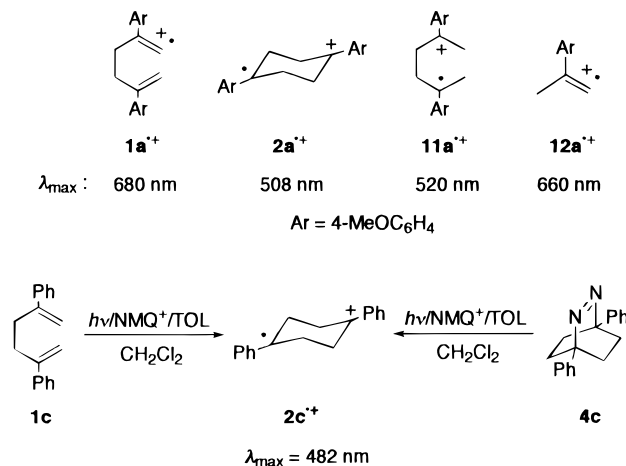
^a $\lambda > 360 \text{ nm}$ irradiation, [1] = 10 mM. ^b [1] = 2 mM.

In contrast, irradiation of DCA with **1a** in oxygen-saturated acetonitrile results in the formation of the oxygenation products 1,4-bis(4-methoxyphenyl)-2,3-dioxabicyclo[2.2.2]octane (**3a**) in 93% yield after 5-min irradiation (Scheme 3). As solvent polarity decreases, yields of oxygenation decrease significantly. In less polar dichloromethane, **3a** is formed in 93% yield after 20-min irradiation, but **1a** is quantitatively recovered even after 60-min irradiation in benzene, in which the degenerate Cope rearrangement efficiently occurs. The electron-donating nature of **1** also affects the efficiency of the oxygenation reaction. As shown in Table 3, the yield of **3** significantly increase with an increase in the electron-donating nature of **1a–d**. Since the CAN- and cerium(IV) tetra-*n*-butylammonium nitrate [Ce(*n*-Bu₄N)₂(NO₃)₆, CBN]¹⁸-catalyzed reaction of **1a** also afforded **3a** together with 4,4'-dimethoxy-*p*-terphenyl (**10a**) under oxygen (Table 4), it is reasonable to conclude that oxygen intercepted CR $2a^{*+}$ in a PET process. By combination of those

(18) Dehmlow, E. V.; Makrandi, J. K. *J. Chem. Res., Synop.* **1986**, 32–33.

Table 4. CAN- or CBN-Catalyzed Oxygenations of **1a** under O₂ and *d*₄-**1a** under N₂ in CH₃CN^a

sub	oxidant	convsn (%)	yields (%)			
			3a	10a	<i>d</i> ₂ - 10a	<i>d</i> ₄ - 1 : <i>d</i> ₄ - 1'
1a	CAN	80	63	9		
1a	CBN	80	58	10		
<i>d</i> ₄ - 1a	CAN	28			4	>99:<1
<i>d</i> ₄ - 1a	CBN	40			5	>99:<1

^a [1] = [*d*₄-1] = 1 mM.**Scheme 4**

experimental results it can be concluded that the PET degenerate Cope rearrangement of *d*₄-**1** occurs in a stepwise mechanism involving the chair^{5,7c} 1,4-diarlylcyclohexane-1,4-diyl CR (*d*₄-**2**⁺). The inverse solvent effects observed in the PET degenerate Cope rearrangement and oxygenation suggest that the degenerate Cope rearrangement preferentially occurs as an in-cage process, while oxygenation occurs as an out-of-cage process.¹⁹

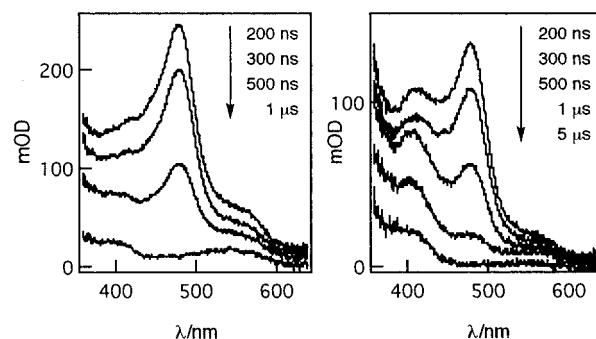
Spectroscopic Identification of 2⁺. In order to observe **2**⁺ spectroscopically, nanosecond laser flash photolysis was carried out for **1a** and **1c** under the DCA- or *N*-methylquinolinium tetrafluoroborate (NMQ⁺BF₄⁻)-sensitized conditions. Upon irradiation (355 nm) of an acetonitrile solution of **1a** (1 mM), DCA (0.35 mM), and biphenyl (BP) (0.2 M) under nitrogen atmosphere, an intense transient absorption with λ_{max} at 508 nm appears after 200 ns. This absorption is assigned to **2a**⁺ by comparison with the absorption maximum of 2,5-bis(4-methoxyphenyl)hexane-2,5-diyl CR (**11a**⁺, λ_{max} = 520 nm in 1,2-dichloroethane) reported by Takamuku and co-workers (Scheme 4).²⁰ CR **2a**⁺ was relatively stable and persisted for several μs under nitrogen at room temperature, but under aerated conditions **2a**⁺ quickly disappeared. A transient absorption due to **1a**⁺, however, could not be observed before **2a**⁺ appeared and after **2a**⁺ disappeared under those conditions. Since our preliminary experiments²¹ of γ-ray irradiation for **1a** in butyl chloride matrix at 77 K exhibited transient absorptions of both **1a**⁺ (λ_{max} = 680 nm)²² and **2a**⁺ (λ_{max} = 520 nm), the CR

(19) Miyashi, T.; Kamata, M.; Mukai, T. *J. Am. Chem. Soc.* **1986**, *108*, 2755–2757. Miyashi, T.; Kamata, M.; Mukai, T. *J. Am. Chem. Soc.* **1987**, *109*, 2780–2788. Hilinski, E. F.; Masnovi, J. M.; Kochi, J. K.; Rentzepis, P. M. *J. Am. Chem. Soc.* **1984**, *106*, 8071–8077. Masnovi, J. M.; Levine, A.; Kochi, J. K. *J. Am. Chem. Soc.* **1985**, *107*, 4356–4358.

(20) Tojo, S.; Toki, S.; Takamuku, S. *J. Org. Chem.* **1991**, *56*, 6240–6243.

(21) Ikeda, H.; Ishida, A.; Takasaki, T.; Tojo, S.; Takamuku, S.; Miyashi, T. *J. Chem. Soc., Perkin Trans. 2* **1997**, 849–850.

(22) The absorption maximum at 680 nm was assigned to **1a**⁺ by the comparison with that of α-methyl-4-methoxystyrene CR (**12a**⁺, λ_{max} = 660 nm in 4:1 water:acetonitrile).²³

**Figure 1.** Nanosecond absorption spectra of an aerated dichloromethane solution of **1c** (1 mM, left) and **4c** (1 mM, right) under the NMQ⁺BF₄⁻ (1 mM)–TOL (2 M) cosensitized conditions.

cyclization of **1a**⁺ to **2a**⁺ in acetonitrile presumably is fast at room temperature.

The laser flash photolysis of **1c** under the NMQ⁺BF₄⁻-sensitized conditions using toluene (TOL) as a cosensitizer in an aerated dichloromethane showed a transient absorption with λ_{max} at 482 nm together with that of NMQ⁺ with λ_{max} at ca. 400 and 550 nm²⁴ (Figure 1). This absorption is assigned to **2c**⁺ by comparison with a transient absorption observed in the laser flash photolysis of **4c** under similar conditions (Scheme 4).²⁵ In favor of this assignment is that the decay rate constant with methanol, *k*_{MeOH}, of the transient intermediate from **1c** (6 × 10⁸ M⁻¹ s⁻¹) is comparable to that from **4c** (8 × 10⁸ M⁻¹ s⁻¹). It is of interest to note that the λ_{max} of **2c**⁺ is significantly red-shifted as compared with those of the cumyl cation (λ_{max} = 326, 390 nm in FSO₃H–SbF₅ at –60 °C)²⁶ and cumyl radical (λ_{max} = 315 nm in cyclohexane),²⁷ suggesting a possible through-bond interaction^{7f} between the cumyl cation and cumyl radical parts of **2c**⁺ in the chair form.

Single-Electron-Transfer Reactions of 4c and d₄-4c under Photoinduced and One-Electron Oxidation Conditions. One possible mechanism for the observed degenerate Cope rearrangement of *d*₄-**1** is a CRCY–CRCL mechanism in which CR *d*₄-**2**⁺ directly undergoes cleavage to form a mixture of *d*₄-**1** and *d*₄-**1'** as shown in Scheme 1c. This mechanism, however, does not account for the failure in cleavage of cyclohexane-1,4-diyl CRs generated by the CAN-catalyzed reaction of **4c**²⁸ and γ-ray irradiations of 1,5-hexadiene,^{29a} bicyclo[2.2.0]-hexane,^{29b} and 2,3-diazabicyclo[2.2.2]oct-2-ene^{29c,d} in Freon matrices. In fact, we also found that the CAN-catalyzed reaction of **1a** in an oxygen-saturated acetonitrile gave **3a** in 63% yield, but the degenerate Cope of *d*₄-**1a** does not occur (Table 4). This result further suggests that *d*₄-**1**⁺ cyclizes to *d*₄-**2**⁺ under both PET and non-PET conditions employed, but *d*₄-**2**⁺ does not

(23) Johnston, L. J.; Schepp, N. P. *J. Am. Chem. Soc.* **1993**, *115*, 6564–6571.

(24) Bockman, T. M.; Kochi, J. K. *J. Am. Chem. Soc.* **1989**, *111*, 4669–4683.

(25) Ikeda, H.; Minegishi, T.; Takahashi, Y.; Miyashi, T. *Tetrahedron Lett.* **1996**, *37*, 4377–4380.

(26) Olah, G. A.; Pittman, C. U., Jr.; Waack, R.; Doran, M. *J. Am. Chem. Soc.* **1966**, *88*, 1488–1495. See: McClelland, R. A.; Chan, C.; Cozes, F.; Modro, A.; Steenken, S. *Angew. Chem., Int. Ed. Engl.* **1991**, *30*, 1337–1339.

(27) Boate, D. R.; Scaiano, J. C. *Tetrahedron Lett.* **1989**, *30*, 4633–4636.

(28) Adam, W.; Grabowski, S.; Miranda, M. A.; Rübenacker, M. *J. Chem. Soc., Chem. Commun.* **1988**, 142–143.

(29) (a) Guo, Q.-X.; Qin, X.-Z.; Wang, J. T.; Williams, F. *J. Am. Chem. Soc.* **1988**, *110*, 1974–1976. (b) Williams, F.; Guo, Q.-X.; Bebout, D. C.; Carpenter, B. K. *J. Am. Chem. Soc.* **1989**, *111*, 4133–4134. (c) Williams, F.; Guo, Q.-X.; Petillo, P. A.; Nelsen, S. F. *J. Am. Chem. Soc.* **1988**, *110*, 7887–7888. (d) Blackstock, S. C.; Kochi, J. K. *J. Am. Chem. Soc.* **1987**, *109*, 2484–2496.

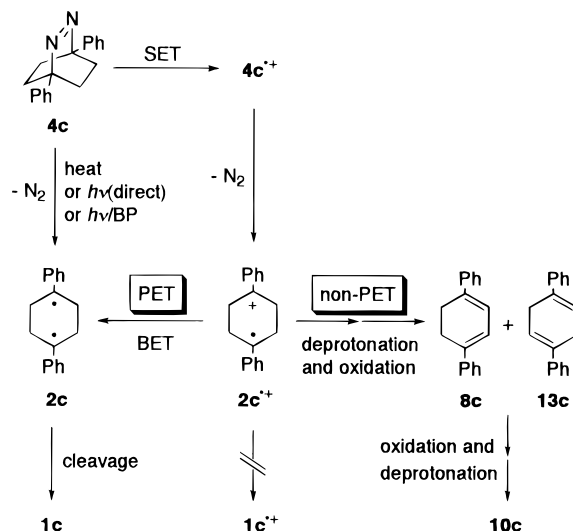
Table 5. Deazetation of **4c** under Various PET^a and Non-PET Conditions

conditions	solvent	conversion (%)	yields (%)	
			1c	10c
PET				
<i>hν</i> /DCA (4 h)	CH ₃ CN	12	12	0
<i>hν</i> /DCA (6 h)	CH ₂ Cl ₂	100	100	0
<i>hν</i> /DCA (2 h)	C ₆ H ₆	100	100	0
<i>hν</i> _{CT} /TCNB (5 h)	CH ₂ Cl ₂	100	100	0
<i>hν</i> _{CT} /TCNE (2 h)	CH ₂ Cl ₂	92	40	0
non-PET				
CAN, <i>n</i> -Bu ₄ NHSO ₄ ^b	CHCl ₃	100	0	46
CBN (1 equiv)	CH ₂ Cl ₂	55	0	18 ^c
(4-BrC ₆ H ₄) ₃ N ⁺ SbCl ₆ ⁻ (2 equiv)	CH ₂ Cl ₂	40	0	29
electrolysis (+1.25 V)	CH ₂ Cl ₂	39	0	11

^a [**4c**] = 0.33 mM (CH₃CN), 10 mM (CH₂Cl₂), or 5 mM (C₆H₆). [DCA] = 1 mM (CH₂Cl₂ and C₆H₆), 0.37 mM (CH₃CN). [TCNB] = [TCNE] = 10 mM. ^b Ref 28. ^c Including the yield for **8c** (11%) and **13c** (3%).

undergo cleavage directly to $d_4\text{-1}^+$ and $d_4\text{-1}'^+$. In contrast, cyclohexane-1,4-diyls undergo facile ring cleavage to give 1,5-hexadienes in pyrolyses¹² and direct photolyses³⁰ of 2,3-diazabicyclo[2.2.2]oct-2-enes. Thus, if a diyl intermediate ($d_4\text{-2}$) is formed by BET from DCA^{•-} to $d_4\text{-2}^+$ under PET conditions, but not under non-PET conditions, then $d_4\text{-1}$ would be expected to undergo the degenerate Cope under PET conditions but not under non-PET conditions. The alternative mechanism including this BET process is a CRCY–DRCL mechanism shown in Scheme 1d, which includes three successive processes; the CR cyclization of $d_4\text{-1}^+$ to $d_4\text{-2}^+$, the BET from DCA^{•-} to $d_4\text{-2}^+$ to form diyl $d_4\text{-2}$, followed by the DR cleavage of $d_4\text{-2}$. The CRCY–DRCL mechanism explains the failure of cyclohexane-1,4-diyl CRs to cleave under non-PET conditions. Apparently, the key step of this mechanism is the BET from DCA^{•-} to $d_4\text{-2}^+$. Thus, it was of particular interest to know whether or not a similar BET process is operative in PET deazetation of **4c**. Deazetations of **4c** were investigated under various PET conditions, and results were compared with those under non-PET conditions.³¹

Irradiation of **4c** with $\lambda > 410\text{-nm}$ light in dichloromethane results in the quantitative recovery of **4c**. However, the DCA-sensitized photoreaction of **4c** with light of similar wavelength quantitatively affords **1c** as shown in Table 5. A solution of **4c** and 1,2,4,5-tetracyanobenzene (TCNB) in dichloromethane exhibits weak and broad charge-transfer (CT) absorption in the visible region over 410 nm. Irradiation of this solution with $\lambda > 410\text{-nm}$ light gives rise to **1c** quantitatively. Similar irradiation of the CT complex of **4c** and tetracyanoethylene (TCNE) ($\lambda_{\text{max}}^{\text{CT}} = 478\text{ nm}$ in dichloromethane) affords **1c** in 40% yield.³² In contrast, like the CAN-catalyzed reaction of

Scheme 5

4c, the CBN-, tris(4-bromophenyl)ammonium hexachloroantimonate³³ [(4-BrC₆H₄)₃N⁺SbCl₆⁻], and anode-catalyzed reactions afforded *p*-terphenyl (**10c**) in low yields, but no **1c**.

Using the oxidation potential of **4c** shown in Table 1, **4c**^{•+} presumably is formed in the DCA-sensitized PET reaction of **4c** as well as non-PET reactions. It is thus reasonable that both PET and non-PET deazetations of **4c** form **2c**^{•+}, and hence, the striking contrast between PET and non-PET reactions of **4c** can be ascribed to differences in the processes following deazetation as shown in Scheme 5.

In non-PET reactions, **2c**^{•+} suffers rapid deprotonation–oxidation processes to form a mixture of 1,4-diphenylcyclohexane-1,3-diene (**8c**) and 1,4-diphenylcyclohexane-1,4-diene (**13c**) and successive one-electron oxidation followed by deprotonation to form **10c**. This was confirmed by the CBN-catalyzed reaction of **4c** which gave a mixture of cyclohexadienes (**8c** and **13c**) along with **10c**, and the (4-BrC₆H₄)₃N⁺SbCl₆⁻-catalyzed oxidation of **8c** afforded **10c** in 70% yield.³⁴ In PET processes, the BET from DCA^{•-}, TCNB^{•-}, or TCNE^{•-} to **2c**^{•+} occurs efficiently to form **2c**, which, in turn, undergoes cleavage to **1c**. Deazetations of **4c** under PET conditions thus provided the same products as those under pyrolytic,¹² direct irradiation³⁰ and benzophenone-sensitized³⁵ reactions in which diyl **2c** is known to serve as a common key intermediate. In fact, BET processes under those PET conditions are energetically favorable. On the basis of reported redox potentials of the cumyl radical ($E^{\text{ox}}_{1/2} = +0.16\text{ V}$ vs SCE in acetonitrile)³⁶ and the electron acceptors ($E^{\text{red}}_{1/2} = -0.95\text{ V}$ for DCA, -0.70 V for TCNB, and $+0.22\text{ V}$ for TCNE), free energy changes, ΔG_{bet} , for BET in the ion radical pair [**2c**^{•+}/acceptor^{•-}] to form **2c** and acceptors are calculated to be -25.5 , -20.7 , and $+1.4\text{ kcal/mol}$, respectively, for DCA, TCNB, and TCNE.³⁷

In non-PET reactions, however, such BET process from Ce^{III} or (4-BrC₆H₄)₃N to **2c**^{•+} are unlikely as calculated free energy changes [$\Delta G_{\text{bet}} = ca. +16.7$ for Ce^{III} and $+20.5\text{ kcal/mol}$ for

(30) Engel, P. S.; Horsey, D. W.; Keys, D. E.; Nalepa, C. J.; Soltero, L. R. *J. Am. Chem. Soc.* **1983**, *105*, 7108–7114.

(31) Ikeda, H.; Minegishi, T.; Miyashi, T. *J. Chem. Soc., Chem. Commun.* **1994**, 297–298.

(32) By control experiments, the low yield of **1c** in the reaction of **4c** and TCNE can be ascribed to the secondary reaction of **1c** with TCNE followed by decomposition.

(33) Reaction of azoalkanes with CR salts: Engel, P. S.; Robertson, D. M.; Scholz, J. N.; Shine, H. J. *J. Org. Chem.* **1992**, *57*, 6178–6187 and references cited therein.

(34) The parent cyclohexane-1,4-diyl CR was reported to undergo a formal 1,3-H shift to give cyclohexene CR.^{29,7f} 1,4-Diphenylcyclohexene, however, was not detected in non-PET reactions of **1c** and **4c**. Since 1,4-diphenylcyclohexene was recovered quantitatively without the formation of **8c** and **13c** in the (4-BrC₆H₄)₃N⁺SbCl₆⁻-catalyzed oxidation, a possible 1,3-H shift pathway can be excluded under the conditions employed.

(35) Adam, W.; Grabowski, S.; H. Platsch; Hannemann, K.; Wirz, J.; Wilson, R. M. *J. Am. Chem. Soc.* **1989**, *111*, 751–753.

(36) Sim, B. A.; Milne, P. H.; Griller, D.; Wayner, D. D. M. *J. Am. Chem. Soc.* **1990**, *112*, 6635–6638.

(4-BrC₆H₄)₃N] indicate. Under PET conditions, a rapid BET³⁸ from DCA^{•-} to 2c^{•+} followed by the ring cleavage of 2c resulted in the formation of 1c. In support of this assumption was the product distribution ratio, *d*₄-1c:*d*₄-1c', from *d*₄-4c under PET and direct irradiation conditions as mentioned later. It is thus reasonably assumed that a similar BET process operates to form *d*₄-2 in the DCA-sensitized PET degenerate Cope of *d*₄-1, completing a CRCY-DRCL mechanism as shown in Scheme 1d.

Photoacoustic Calorimetric Analysis and Energetics of the PET Degenerate Cope Rearrangement of *d*₄-1. The direct CR cleavage of *d*₄-2^{•+} to *d*₄-1^{•+} and *d*₄-1'^{•+} does not compete with BET from DCA^{•-} to *d*₄-2^{•+}. A possible kinetic reason for this observation is based on the reaction thermodynamics. To determine the energetics of the CR cleavage, the enthalpy of formation, Δ*H*_{irp}([2^{•+}/DCA^{•-}]), of the ion radical pair [2^{•+}/DCA^{•-}] must be measured. For this, we applied nanosecond time-resolved photoacoustic calorimetry (PAC), which is a useful technique to determine energetics of various PET reactions as have been reported previously.⁴⁰ The deconvolution of the experimental acoustic waveforms can provide the amplitude and time evolution of heat that is emitted when the excited sensitizer affords [2^{•+}/sensitizer^{•-}]. Experiments were performed for both the 1a-c-DCA-BP and 1c-NMQ⁺PF₆⁻-TOL systems in acetonitrile according to the reported procedure.⁴¹ In Figure 2, a schematic diagram for PAC is described for the 1-DCA-BP system. Enthalpy of formation of [2^{•+}/DCA^{•-}] can be expressed by eqs 1 and 2

$$\Delta H_{\text{irp}}([2^{\bullet+}/\text{DCA}^{\bullet-}]) = h\nu(1 - \alpha_1 - \alpha_2)/\phi \quad (1)$$

$$\phi = h\nu(1 - \alpha_1)/E([\text{BP}^{\bullet+}/\text{DCA}^{\bullet-}]) \quad (2)$$

where *hν*, φ, and *E*([BP^{•+}/DCA^{•-}]) are photon energy (415 nm, 68.9 kcal/mol), the quantum yield to form [BP^{•+}/DCA^{•-}], and the energy (66.2 kcal/mol) of [BP^{•+}/DCA^{•-}] determined from redox potentials of BP and DCA, respectively.

(37) This calculation has been done on the assumption that *E*^{ox}_{1/2} of 2c is comparable with that of the cumyl radical. As one of the reviewers pointed out, this estimation of Δ*G*_{bet} gives a lower limit because the *E*^{ox}_{1/2} of 2c may be more negative. This was suggested from a significant electron coupling between the cumyl cation and cumyl radical parts in 2c^{•+} that cause the remarkable red shift of 2c^{•+} in the electronic absorption spectroscopy. Unfortunately, however, it is difficult to evaluate the effect of through-bond interaction upon redox potentials.

(38) By using the following equations (3, 4)³⁹ and reported parameters by Farid^{15c} and Kikuchi,^{15d} rate constant, *k*_{bet}, of the BET in [2c^{•+}/DCA^{•-}] at 20 °C was estimated to be 1.9 × 10⁹ s⁻¹ and 4.9 × 10¹⁰ s⁻¹, respectively, in acetonitrile

$$k_{\text{bet}} = \left(\frac{4\tau^3}{h^2\lambda_s k_b T} \right)^{1/2} |V|^2 \sum_{\omega=0}^{\infty} \left(\frac{e^{-S} S^\omega}{\omega!} \right) \exp \left\{ - \frac{(\lambda_s + \Delta G_{\text{bet}} + \omega h\nu)^2}{4\lambda_s k_b T} \right\} \quad (3)$$

$$S = \lambda_s / h\nu \quad (4)$$

where parameters |*V*|², λ_s, λ_v, and ν are, respectively, an electronic matrix element squared, solvent reorganization energy, vibrational reorganization energy, and single average frequency.

(39) Miller, J. R.; Beitz, J. V.; Huddleston, R. K. *J. Am. Chem. Soc.* **1984**, *106*, 5057–5068. Siders, P.; Marcus, R. A. *J. Am. Chem. Soc.* **1981**, *103*, 741–747, 748–752. Van Duyne, R. P.; Fischer, S. F. *Chem. Phys.* **1974**, *5*, 183–197. Ulstrup, J.; Jortner, J. *J. Chem. Phys.* **1975**, *63*, 4358–4368.

(40) Rothberg, L. J.; Simon, J. D.; Bernstein, M.; Peters, K. S. *J. Am. Chem. Soc.* **1983**, *105*, 3464–3468. Goodman, J. L.; Peters, K. S. *J. Am. Chem. Soc.* **1986**, *108*, 1700–1701. Ci, X.; da Silva, R. S.; Goodman, J. L.; Nicodem, D. E.; Whitten, D. G. *J. Am. Chem. Soc.* **1988**, *110*, 8548–8550. Zona, T. A.; Goodman, J. L. *Tetrahedron Lett.* **1992**, *33*, 6093–6096. LaVilla, J. A.; Goodman, J. L. *J. Am. Chem. Soc.* **1989**, *111*, 712–714.

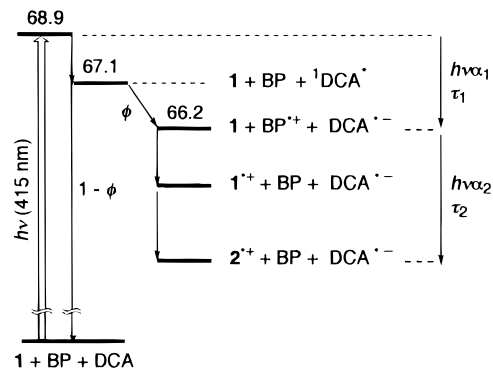


Figure 2. Schematic diagram of PAC for the 1-DCA-BP system.

From several experiments, the deconvolution parameters, α₁, α₂, and τ₂ are determined to be 0.29 ± 0.03, 0.24 ± 0.05, and 194 ± 42 ns, respectively, for the 1c-DCA-BP system. Δ*H*_{irp}([2a-c^{•+}/DCA^{•-}]), i.e., energy difference between [2a-c^{•+}/DCA^{•-}] and the ground states of 1a-c and DCA, were thus determined to be 40.8 ± 5.3, 44.2 ± 5.4 and 43.6 ± 4.5 kcal/mol for 2a, 2b, and 2c, respectively.⁴² For the 1c-NMQ⁺PF₆⁻-TOL system, the deconvolution parameters, α₁, α₂, and τ₂ were determined to be 0.57 ± 0.02, 0.27 ± 0.03, and 180 ± 55 ns, respectively. From those values and numerous calibrations, energy of the ion-radical pair [2c^{•+}/NMQ⁺PF₆⁻] was given by the equation Δ*H*_{irp}([2c^{•+}/NMQ⁺PF₆⁻]) = *hν* × (1 - α₁) + 9 kcal/mol.⁴³ Using the α₁ value and photon energy (337 nm, 84.8 kcal/mol), Δ*H*_{irp}([2c^{•+}/NMQ⁺PF₆⁻]) was determined to be 45.6 ± 3.5 kcal/mol. The reliability of Δ*H*_{irp} values determined for both systems was verified by taking into account the difference (0.05 V) in *E*^{red}_{1/2} between DCA¹⁴ and NMQ⁺PF₆⁻ (-0.90 V vs SCE in acetonitrile). Energy of the ion radical pair Δ*H*_{irp}([2c^{•+}/NMQ⁺PF₆⁻]) can be compared with that of [2c^{•+}/DCA^{•-}] by adding 1.2 kcal/mol. The resulting energy of the ion-radical pair, 46.8 ± 3.5 kcal/mol, approximates to 43.6 ± 4.5 kcal/mol within experimental errors. After all, Δ*H*_{irp}([2c^{•+}/DCA^{•-}]) was determined statistically to be 44.4 ± 4.5 kcal/mol as shown in Figure 3.

By using the redox potentials of 1c and DCA, the free energy changes of the formation of [1c^{•+}/DCA^{•-}] are calculated to be 60.6 kcal/mol. On the basis of our results²¹ of pulse radiolysis for cyclization of *d,l*-2,5-bis(4-methoxyphenyl)-3,4-dimethyl-1,5-hexadiene CR to *trans*-1,4-bis(4-methoxyphenyl)-2,3-dimethylcyclohexane-1,4-diyl CR, the enthalpy of activation for cyclization of 1c^{•+} to 2c^{•+} was assumed to be 3~4 kcal/mol. The energy barrier for the CR cleavage of 2c^{•+} is thus >19 kcal/mol as shown in Figure 3. This barrier seems to be too high for *d*₄-1c to undergo the degenerate Cope, especially at -80 °C, in a CRCY-CRCL mechanism, and hence, 2c^{•+} enters into the DR energy surface through the competing exothermic BET process. Because Δ*H*_{irp}([2c^{•+}/DCA^{•-}]) and the Δ*G*_{bet} for the BET from DCA^{•-} to 2c^{•+} are ca. 44.4 ± 4.5 and ca. 25.6 kcal/mol, respectively, diyl 2c will lie ca. 18.8 kcal/mol higher in energy than 1c and ca. 25.6 kcal/mol below [2c^{•+}/DCA^{•-}].³⁷ The experimental PAC results demonstrate the endothermicity⁴

(41) Rudzki, J. E.; Goodman, J. L.; Peters, K. S. *J. Am. Chem. Soc.* **1985**, *107*, 7849–7854. Herman, M. S.; Goodman, J. L. *J. Am. Chem. Soc.* **1989**, *111*, 1849–1854. Peters, K. S. In *Kinetics and Spectroscopy of Carbenes and Biradicals*; Platz, M. S., Ed.; Plenum: New York, 1990; pp 37–49. Griller, D.; Wayner, D. D. M. *Pure Appl. Chem.* **1989**, *61*, 717–724.

(42) Similarly, Δ*H*_{irp}([2c^{•+}/NMQ⁺PF₆⁻]) in 1,2-dichloroethane was determined to be 45.1 ± 2.3 kcal/mol by using the following parameters; α₁ = 0.32 ± 0.02, α₂ = 0.27 ± 0.02, and τ₂ = 233 ± 36 ns (averages from five runs).

(43) Goodman, J. L. unpublished results.

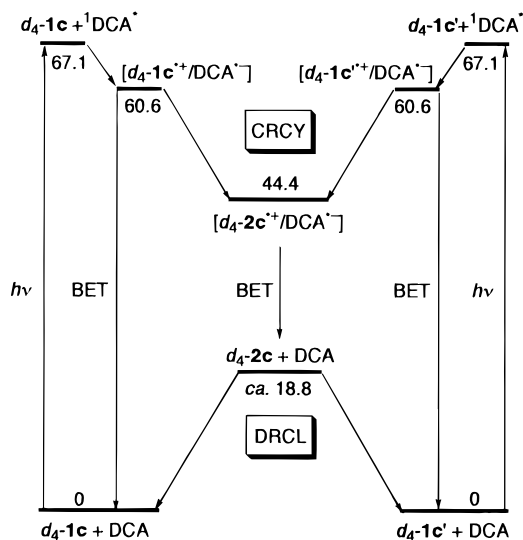
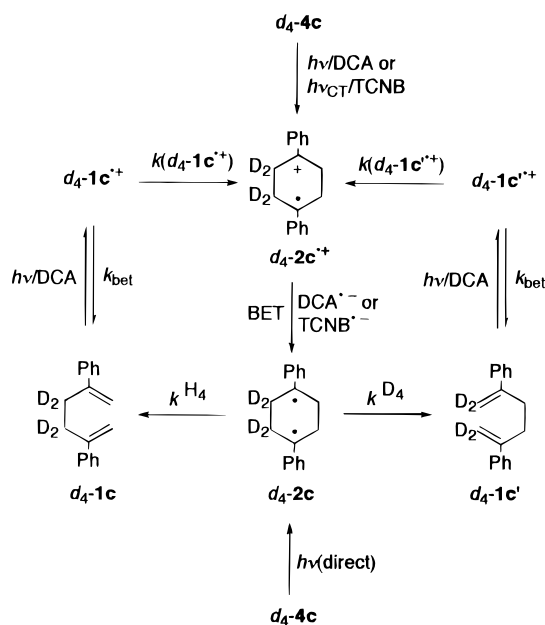


Figure 3. Energy diagram for the DCA-sensitized PET degenerate Cope rearrangement of $d_4\text{-1c}$. Relative energy was represented in kcal/mol.

Scheme 6



of the direct CR cleavage of $d_4\text{-2c}^+$ to $d_4\text{-1c}^+$ and $d_4\text{-1c}'^+$, which allows competitive BET to form $d_4\text{-2c}$.

Bond-Breaking and Bond-Making Kinetic Isotope Effects on a CRCY–DRCL Mechanism. In order to gain further insight into a CRCY–DRCL mechanism, we investigated deazetations of $d_4\text{-4c}$ under various photochemical conditions. If a CRCY–DRCL mechanism is really operative in the PET degenerate Cope of $d_4\text{-1c}$, the observed PS ratio, $[d_4\text{-1c}]_{\text{ps}}/[d_4\text{-1c}']_{\text{ps}} = \text{ca. } 52/48$, can be expressed by $[\Phi(d_4\text{-1c}^+)/\Phi(d_4\text{-1c}'^+)] \times [k^{\text{H4}}/k^{\text{D4}}]$, where $\Phi(d_4\text{-1c}^+) = k(d_4\text{-1c}^+)/[k(d_4\text{-1c}^+) + k_{\text{bet}}]$ and $\Phi(d_4\text{-1c}'^+) = k(d_4\text{-1c}'^+)/[k(d_4\text{-1c}'^+) + k_{\text{bet}}]$ (Scheme 6). The former is a ratio of the efficiency of the CRCY step in an ion-radical pair, whereas the latter corresponds to the bond-breaking kinetic isotope effects (DR–BBKIE) of the DRCL step. Thus, the direct determination of the DR–BBKIE of $d_4\text{-2c}$ by independent generation would provide the efficiency ratio $\Phi(d_4\text{-1c}^+)/\Phi(d_4\text{-1c}'^+)$ and judge which step controls the PS ratio. Furthermore, if a mechanism for the PET deazetation of

Table 6. Deazetation of $d_4\text{-4c}$ under PET and Direct Irradiation Conditions at 20 °C^a

conditions	relative yields (%)		$k^{\text{H4}}/k^{\text{D4}}$
	$d_4\text{-1c}$	$d_4\text{-1c}'$	
$h\nu/\text{DCA}/\text{CD}_2\text{Cl}_2^b$	52.5 ± 0.3	47.5 ± 0.3	1.10 ± 0.02
$h\nu_{\text{CT}}/\text{TCNB}/\text{CD}_2\text{Cl}_2^c$	52.3 ± 0.4	47.7 ± 0.4	1.10 ± 0.02
$h\nu(\text{direct})/\text{C}_6\text{D}_6^d$	52.6 ± 0.3	47.4 ± 0.3	1.11 ± 0.02

^a The errors are 1 σ . ^b $\lambda > 410$ nm, 12–32% conversion. ^c $\lambda > 410$ nm, 10–28% conversion. ^d $\lambda > 320$ nm, 45–100% conversion.

4c includes BET to form diyl **2c**, the product distribution ratio, $d_4\text{-1c}:d_4\text{-1c}'$, in the PET deazetation of $d_4\text{-4c}$ should be same as that in direct photolysis of $d_4\text{-4c}$ as described in Scheme 6.

As shown in Table 6, the distribution ratio, $d_4\text{-1c}:d_4\text{-1c}'$, under direct irradiation conditions was nearly same as not only that under PET conditions but also the PS ratio of the PET degenerate Cope of $d_4\text{-1c}$. This observation is reasonable if the PET degenerate Cope of $d_4\text{-1c}$ occurs in a CRCY–DRCL mechanism involving $d_4\text{-2c}^+$ and $d_4\text{-2c}$ and deazetation of $d_4\text{-4c}$ forms $d_4\text{-2c}$ as a common intermediate in a cleavage step under the PET and direct irradiation conditions (Scheme 6). From the distribution ratio ($d_4\text{-1c}:d_4\text{-1c}' = 52.6:47.4$ at 20 °C) observed in direct irradiation of $d_4\text{-4c}$ and the PS ratio ($d_4\text{-1c}:d_4\text{-1c}' = 52.4:47.6$ at 20 °C) of the PET degenerate Cope of $d_4\text{-1c}$, the efficiency ratio $\Phi(d_4\text{-1c}^+)/\Phi(d_4\text{-1c}'^+)$ and DR–BBKIE can be calculated to be 0.99 and 1.11, respectively, at 20 °C. The fact that the distribution ratio from $d_4\text{-2c}$ is nearly same as the PS ratio of the PET degenerate Cope of $d_4\text{-1c}$ suggests that the DRCL step predominates the determination of the PS ratio of the PET Cope of $d_4\text{-1c}$. In fact, the bond-making kinetic isotope effects (CR–BMKIE) of the CRCY step is substantially 1.0, because $k(d_4\text{-1c}^+) = k(d_4\text{-1c}'^+)$ when $\Phi(d_4\text{-1c}^+)/\Phi(d_4\text{-1c}'^+) = 0.99$. This indicates that there is no inverse KIE for the $\text{sp}^2 \rightarrow \text{sp}^3$ bond-making step. A plausible explanation will be that a highly exothermic CRCY process with low activation energy proceeds through an early transition state in which the σ (C-3–C-4) bond is kept intact and C-1 and C-6 keep the sp^2 -like character of $d_4\text{-1c}^+$ (or $d_4\text{-1c}'^+$). In this sense, of importance is an intramolecular charge-transfer interaction^{7c} between the neutral styrene unit as an electron donor and the styrene CR unit as an electron acceptor in 1c^+ . Both the CR–BMKIE and DR–BBKIE thus explain consistently the PS ratio of the PET degenerate Cope of $d_4\text{-1c}$ if a CRCY–DRCL mechanism is operative.

Conclusions

The operation of the CRCY–DRCL mechanism is established for the DCA-sensitized PET degenerate Cope rearrangement of $d_4\text{-1}$. This mechanism avoids the proposed endothermicity⁴ of the direct CR cleavage of $d_4\text{-2}^+$ in a CRCY–CRCL mechanism and accounts for differences in the reactivity of $d_4\text{-2}^+$ formed under PET and non-PET conditions. Accordingly, an exothermic BET process to form a low-lying diyl $d_4\text{-2}$ is an important key process in PET conditions. Significant solvent effects on quantum efficiencies (Table 2) are in accord with a probable operation of the CRCY–DRCL mechanism in which BET in $[2^+/\text{DCA}^-]$ efficiently operates. In connection with the directly determined DR–BBKIE of $d_4\text{-2c}$, it is of particular interest to note that the value, 1.11, is very close to the BBKIE, 1.07, determined kinetically by Gajewski for the thermal degenerate Cope of $d_4\text{-1c}$ through a six-membered cyclic

transition state.⁴⁴ Interestingly, the calculations of Dewar suggested that the kinetically determined BBKIE, 1.07, can be reproducible as the BBKIE of *d*₄-**2c** in a stepwise CY–CL mechanism described in Scheme 1a.^{3f} Of course, the DR–BBKIE determined directly from *d*₄-**2c** in this work cannot simply judge whether *d*₄-**2c** is a putative or true intermediate in the thermal degenerate Cope of *d*₄-**1c**. Nevertheless, the direct determination of DR–BBKIE and experimental energy evaluation of *d*₄-**2c** would be of basic value for further argument on a mechanism of the thermal degenerate Cope of *d*₄-**1c**. A mechanistic connection between CR and DR in the PET reaction is another intriguing aspect. If an efficient BET from a sensitizer anion radical to an intermediate CR is operative, the PET reaction is a useful mechanistic probe to investigate intriguing but unobservable reactive diyl intermediates in thermal reactions.

Experimental Section

General Methods. All melting and boiling points are uncorrected. Elemental analyses were performed by the Instrumental Analyses Center for Chemistry, Graduate School of Science, Tohoku University, and correct elemental analyses were obtained for all new compounds in this report. ¹H NMR spectra were recorded at 90 MHz on a Varian EM-390, at 200 MHz on a Varian XL-200, or at 400 MHz on a JEOL GX-400 spectrometer. Chemical shifts were reported by using the following abbreviations: s, singlet; d, doublet; t, triplet; q, quartet; m, multiplet; br, broad; J, coupling constants (Hz). Product analyses by ¹H NMR were done using 1,1,2,2-tetrachloroethane or 1,1,1,2-tetrachloroethane as an internal standard. ¹³C NMR spectra were obtained at 50 MHz on a Varian XL-200 spectrometer. MS were performed on a Hitachi M-52, a JEOL JMS-HX110, or a Hitachi M-2500 mass spectrometer under electron ionization. Redox potentials (*E*^{ox}_{1/2} and *E*^{red}_{1/2}; V vs SCE) were measured on a Yanaco P-1000 voltammetric analyzer by cyclic voltammetry (Pt electrode, scan rate 100 mV/s) in CH₃CN containing Et₄NClO₄ (0.1 M) as a supporting electrolyte. Because all of substrates gave irreversible waves, their *E*^{ox}_{1/2} values were obtained as *E*_{ap} (anodic peak potential) – 0.03 V, assuming a one-electron oxidation process. Fluorescence spectra were recorded on a Hitachi MPF-4 or on a Hitachi F-4010 fluorescence spectrophotometer. Nanosecond absorption spectroscopy was carried out by using a Continuum Surelite-10 YAG laser system (Nd, THG, λ_{ex} = 355 nm, 55 mJ) for the DCA–BP cosensitization or Lumonics EX600 excimer laser (XeCl, λ_{ex} = 308 nm, 100 mJ) for the NMQ⁺BF₄[–]–TOL cosensitization and a pulsed Xe arc lamp (150 W) as a monitoring light source. A PRA nitrogen laser LN 1000 was used for photoacoustic calorimetry experiments done in the NSF Center for Photoinduced Charge Transfer at the University of Rochester. Ethereal solvents were dried and distilled from LiAlH₄. CH₃CN was dried and distilled from P₂O₅ and then CaH₂. C₆H₆ and CH₂Cl₂ were dried and distilled from CaH₂. Deuterated solvents for photoreactions, CD₃CN (99.6% deuterated), C₆D₆ (99.6%), CD₃C₆D₅ (99.6%), and CD₂Cl₂ (99.3%) were dried over molecular sieves 4A prior to use. Merck silica gel 60 (230–400 mesh) was used for column chromatography. Aminium salt, (4-BrC₆H₄)₃N⁺SbCl₆[–], (Aldrich) was washed with dry ether and dried in vacuo prior to use. Preparative thick-layer chromatography (PTLC) was performed on 0.5 mm × 20 cm × 20 cm plates (E. Merck, silica gel 60 PF₂₅₄).

Syntheses of Substrates Shown in Scheme 2. See the Supporting Information.

DCA Fluorescence Quenching. The DCA fluorescence quenching experiments were carried out under air, monitoring the changes in the intensity of fluorescence at λ_{max} = ca. 436 and 460 nm as a function of concentration of quencher. The slope of *I*⁰/*I* vs [quencher] in the Stern–Volmer plot, which equals *k*_qτ, was determined by the least-squares method. Quenching efficiencies, *Q*_c, at [I] = 10 mM and

Table 7. Quenching Efficiencies (*Q*_c) for ¹DCA* with **1** and Quantum Yields (Φ) for the PET Degenerate Cope Rearrangements of *d*₄-**1** at 20 °C^a

sub	<i>Q</i> _c			sub	Φ		
	CD ₃ CN	CD ₂ Cl ₂	C ₆ D ₆		CD ₃ CN	CD ₂ Cl ₂	C ₆ D ₆
1a	0.732	0.644	0.545	<i>d</i> ₄ - 1a	n.a. ^b	0.088	0.21
1b	0.662	0.543	0.361	<i>d</i> ₄ - 1b	0.14	0.18	0.17
1c	0.623	0.295	0.0616	<i>d</i> ₄ - 1c	0.21	0.13	0.031
1d	0.595	0.249	0.0293	<i>d</i> ₄ - 1d	0.20	0.089	0.010

^a [I] = [*d*₄-**1**] = 10 mM. ^b No attempt.

quenching rate constants, *k*_q, calculated from known τ are shown in Tables 7 and 1, respectively.

Analyses of Time-Dependent Change of Product Ratios for the DCA-Sensitized Photoreactions of *d*₄-1a–d** and **4c**.** A typical procedure: A 0.1 M solution (0.5 mL) containing 0.05 mmol of *d*₄-**1c** or **4c** and 2–3 mg of DCA in CD₃CN, CD₂Cl₂, or C₆D₆ was irradiated with a 2 kW Xe lamp through a Toshiba cutoff filter L-39 (λ > 360 nm) for *d*₄-**1c** or Y-44 (λ > 410 nm) for *d*₄-**4c** under N₂ at 20 ± 1 °C. Taking into account the 98% deuterium incorporation in *d*₄-**1c**, the *d*₄-**1c**:*d*₄-**1c'** ratios in the photoreaction of *d*₄-**1c** were determined by 200 MHz ¹H NMR analyses as follows: *d*₄-**1c**:*d*₄-**1c'** = (*I*₁ – α):(*I*₂ – α), α = (*I*₁ + *I*₂) – (*I*₁ + *I*₂)/1.02, where *I*₁ and *I*₂ are integration intensities of olefin protons (2 H + 2 H) (*d*₄-**1c**: δ 5.05 and 5.28 in CDCl₃) and methylene protons (4 H) (*d*₄-**1c**: δ 2.65 in CDCl₃), respectively. Similarly, the *d*₄-**4c**:*d*₄-**1c**:*d*₄-**1c'** ratios in the photoreaction of *d*₄-**4c** (97% deuteration) were determined by 200 MHz ¹H NMR analyses as follows: *d*₄-**4c**:*d*₄-**1c**:*d*₄-**1c'** = *I*₃ / 1.03:(*I*₁ – α):(*I*₂ – α), where *I*₃ is integration intensities of methylene protons (2 H + 2 H) (δ 1.53 and 2.20 in CDCl₃), α = (*I*₁ + *I*₂) – (*I*₁ + *I*₂)/1.03. Results are shown in Table 2.

Quantum Yield Determinations. A typical procedure: A CH₃CN, CH₂Cl₂, or C₆H₆ solution (3 mL) containing 0.03 mmol of *d*₄-**1c** (10 mM) and DCA (0.19 mM in CH₃CN; 0.47 mM in CH₂Cl₂; or 0.68 mM in C₆H₆) was irradiated with light of wavelength at λ_{max} = 368 ± 24 nm under N₂ at 20 ± 1 °C. Light of this wavelength was obtained from a 500 W Hg–Xe lamp through an aqueous CuSO₄ solution filter, a Toshiba cutoff filter UV-35, and an interference filter (λ_{max} = 363 nm). Aberchrome 540 was used as an actinometer. The conversion was 5–15% in all cases. After irradiation and removal of solvent in the dark, the photolysate was analyzed by ¹H NMR. Thus, there is at least ca. 2% of the experimental error in each case. Taking into account the 98% deuterium incorporation, the true conversion percentage, *C* (%), was determined as *C* (%) = [1.02 × [*I*₂/(*I*₁ + *I*₂)] – 0.02]/0.98 × 100. Uncorrected Φ and corrected Φ_{cor} are summarized in Tables 7 and 2, respectively.

DCA-Sensitized Photoreactions of **1a–d under O₂.** A typical procedure: A 5 mL solution containing 0.05 mmol of **1c** (0.01 M) and 2–3 mg of DCA in CH₃CN, CH₂Cl₂, or C₆H₆ was irradiated with a 2 kW Xe lamp through a Toshiba cutoff filter L-39 (λ > 360 nm) under O₂ at 20 ± 1 °C. Removal of solvent, PTLC, followed by recrystallization from CH₂Cl₂–ether afforded cyclic peroxide **3c**. Results are shown in Table 3. Physical data for **3a–d** are shown in the Supporting Information.

Photoreaction of **4c in the Absence of DCA with Wavelength λ > 400 nm and Reaction of **4c** in the Presence of DCA in the Dark.** A 5 mL C₆H₆ solution containing 6.6 mg (0.025 mmol) of **4c** was irradiated for 2 h with a 2 kW Xe lamp through a Toshiba cutoff filter Y-44 (λ > 410 nm) under N₂ at 20 ± 1 °C. Removal of C₆H₆ and ¹H NMR analysis showed the quantitative recovery of **4c**. Similarly, a 5 mL CH₂Cl₂ solution containing 13.1 mg (0.05 mmol) of **4c** was irradiated for 10 h. ¹H NMR analysis showed only 2% conversion of **4c** to **1c**. A 5 mL CH₂Cl₂ solution containing 13.1 mg (0.05 mmol) of **4c** was stirred under N₂ at 20 ± 1 °C in the dark. Removal of CH₂Cl₂ and ¹H NMR analysis showed the quantitative recovery of **4c**.

DCA-Sensitized Photoreaction of **4c.** A solution of **4c** (13.1 mg, 0.05 mmol) and DCA (7.7 mg, 0.034 mmol) in CH₃CN (150 mL) was irradiated with a 2 kW Xe lamp through a Toshiba cutoff filter Y-44 (λ > 410 nm) under N₂ at 20 ± 1 °C. Removal of solvent followed by PTLC afforded **1c** quantitatively. Similarly, **1c** was quantitatively

(44) (a) Gajewski, J. J.; Conrad, N. D. *J. Am. Chem. Soc.* **1978**, *100*, 6269–6270. (b) Gajewski, J. J.; Conrad, N. D. *J. Am. Chem. Soc.* **1979**, *101*, 6693–6704. (c) Gajewski, J. J. *Acc. Chem. Res.* **1980**, *13*, 142–148. (d) Gajewski, J. J. *Hydrocarbon Thermal Isomerization*; Academic: New York, 1981.

afforded upon irradiation of a 5 mL CH₂Cl₂ or C₆H₆ solution containing **4c** (13.1 mg, 0.05 mmol in CH₂Cl₂ or 6.6 mg, 0.025 mmol in C₆H₆) and DCA (1.1 mg, 0.005 mmol).

Photoexcitation of the CT Complex of 4c and TCNB. A 5 mL CH₂Cl₂ solution containing 13.1 mg (0.05 mmol, 0.01 M) of **4c** and 8.9 mg (0.05 mmol) of TCNB was irradiated for 5 h with a 2 kW Xe lamp through a Toshiba cutoff filter Y-44 ($\lambda > 410$ nm) under N₂ at 20 ± 1 °C. Removal of solvent followed by PTLC afforded **1c** quantitatively and ¹H NMR analysis showed the quantitative recovery of TCNB.

Photoexcitation of the CT Complex of 4c and TCNE. A 5 mL CH₂Cl₂ solution containing 13.1 mg (0.05 mmol, 0.01 M) of **4c** and 6.4 mg (0.05 mmol) of TCNE was irradiated for 2 h with a 2 kW Xe lamp through a Toshiba cutoff filter Y-44 ($\lambda > 410$ nm) under N₂ at 20 ± 1 °C. Removal of solvent followed by ¹H NMR analysis showed the formation of **1c** (40%) along with the recovered **4c** (8%). The recovery of TCNE in photolysate was determined to be 28% by the reaction of TCNE and α -terpinene which occurs quantitatively.

CAN-Catalyzed Reaction of 1a under O₂. A two-necked flask containing a solution of **1a** (14.7 mg, 0.05 mmol) in dry CH₃CN (50 mL) was replaced with O₂. To this solution, CAN (27.4 mg, 0.05 mmol) was added in one portion under stirring and the mixture was stirred for 20 min. After addition of water, the reaction mixture was extracted with ether. The combined extract was washed with water and brine and dried over Na₂SO₄. Removal of solvent followed by PTLC afforded **3a** (63%) and **10a** (9%) along the recovered **1a** (20%).

CBN-Catalyzed Reaction of 1a under O₂. A two-necked flask containing a solution of **1a** (29.4 mg, 0.1 mmol) in dry CH₃CN (100 mL) was replaced with O₂. To this solution was added CBN (99.7 mg, 0.1 mmol) in one portion under stirring, and the mixture was stirred for 30 min. The same workup as that for the CAN-catalyzed reaction of **1a** under O₂ followed by PTLC afforded **3a** (58%) and **10a** (10%) along with the recovered **1a** (20%).

CAN-Catalyzed Reaction of d₄-1a under N₂. A two-necked flask containing a solution of d₄-**1a** (14.9 mg, 0.05 mmol) in dry CH₃CN (50 mL) was replaced several times with N₂. To this solution was added CAN (27.4 mg, 0.05 mmol) in one portion, and the mixture was stirred for 20 min under N₂. After addition of water, the reaction mixture was extracted with ether. The same workup as that for the CAN-catalyzed reaction of **1a** under O₂ followed by ¹H NMR analysis showed the formation of 2',3'-dideuterio-4,4''-dimethoxy-*p*-terphenyl (d₂-**10a**) (4%) along with the recovered d₄-**1a** (72%).

CBN-Catalyzed Reaction of d₄-1a under N₂. A two-necked flask containing a solution of d₄-**1a** (14.9 mg, 0.05 mmol) in dry CH₃CN (50 mL) was replaced several times with N₂. To this solution was added CBN (54.7 mg, 0.05 mmol) in one portion, and the mixture was stirred for 1 h under N₂. After addition of water, the reaction mixture was extracted with ether. The same workup as that for the CAN-catalyzed reaction of **1a** under O₂ followed by ¹H NMR analysis showed the formation of d₂-**10a** (5%) along with the recovered d₄-**1a** (60%).

CBN-Catalyzed Reaction of 4c under N₂. A two-necked flask containing a solution of diazene **4c** (13.1 mg, 0.05 mmol) in dry CH₂-

Cl₂ (5 mL) was replaced several times with N₂. To this solution was added CBN (54.7 mg, 0.05 mmol) in one portion, and the mixture was stirred for 1 h under N₂. After addition of water, the reaction mixture was extracted with CH₂Cl₂. The same workup as that for the CAN-catalyzed reaction of **1a** under O₂ followed by ¹H NMR analysis showed the formation of **7c** (11%), **10c** (4%), and **13c** (3%) along with recovered **4c** (45%).

(4-BrC₆H₄)₃N⁺SbCl₆⁻-Catalyzed Reaction of 4c under N₂. A two-necked flask containing diazene **4c** (13.1 mg, 0.05 mmol) in CH₂-Cl₂ (5 mL) was replaced several times with N₂. To this solution was added (4-BrC₆H₄)₃N⁺SbCl₆⁻ (40.8 mg, 0.05 mmol) in one portion, and the mixture was stirred under N₂. When the blue color of aminium salt faded, aminium salt was added twice (20.4 mg each) further, and the reaction mixture was stirred for 1 h. After addition of 28% NaOMe/MeOH (1 mL) and water, the mixture was extracted with CH₂Cl₂. The same workup as that for the CAN-catalyzed reaction of **1a** under O₂ followed by ¹H NMR analysis showed the formation of **10c** (29%) along with the recovered **4c** (60%).

Electrode-Catalyzed Reaction of 4c. A CH₂Cl₂ solution (20 mL) containing 13.1 mg (0.05 mmol) of diazene **4c** and 0.05 M Et₄NClO₄ in an electrolytic cell was subjected to the anodic oxidation on a Pt electrode at +1.25 V under N₂ for 18 h. A saturated calomel electrode (SCE) was used as a reference electrode. Washing with water, drying over Na₂SO₄, removal of solvent followed by ¹H NMR analysis showed the formation of **10c** (11%) along with the recovered **4c** (61%).

Direct Irradiation of d₄-4c. A 5 mL C₆H₆ solution containing 6.7 mg (0.025 mmol) of d₄-**4c** was irradiated for 5 h with a 2 kW Xe lamp through a Toshiba cutoff filter UV-35 ($\lambda > 320$ nm) under N₂ at 20 ± 1 °C. The d₄-**1c**:d₄-**1c'** ratios were determined by 200 MHz ¹H NMR analyses (*vide supra*).

Energy Determination by Time-Resolved PAC. The details of the PAC experiment has been described previously.⁴¹ A chart of the PAC waveforms for **1c**-DCA-BP system and lists of deconvolution fitting parameters for experimental waveforms in each PAC experiment are shown in the Supporting Information. Values were obtained by at least three separate runs, and errors are within 1 σ .

Acknowledgment. We acknowledge financial support from the Ministry of Education, Science, Sports and Culture (Grant-in-Aid for Nos. 05044212, 06453032, 06740544, 06044014, and 06239106). We also thank Professors J. A. Berson and J. P. Dinnocenzo for valuable discussions.

Supporting Information Available: Synthetic details of Scheme 2, PAC experiment, a chart of the PAC waveforms for the **1c**-DCA-BP system, and lists of deconvolution fitting parameters for experimental waveforms in each PAC experiment (13 pages). See any current masthead page for ordering and Internet access instructions.

JA971910S